Imaging Glycosylation

ARTICLE *in* JOURNAL OF THE AMERICAN CHEMICAL SOCIETY · AUGUST 2008

Impact Factor: 12.11 · DOI: 10.1021/ja802535p · Source: PubMed

J|A|C|S
COMMUNICATIONS

Published on Web 06/05/2008

Imaging Glycosylation

Hongda Wang,[†] Linda Obenauer-Kutner,[||] Mei Lin,[||] Yunping Huang,[||] Michael J. Grace,[||] and Stuart M. Lindsay*[,†,‡,§]

Center for Single Molecule Biophysics, The Biodesign Institute, Department of Chemistry and Biochemistry, Department of Physics, Arizona State University, Tempe, Arizona 85287-1604, and Protein Therapeutics Development, Bioanalytical Sciences, Bristol-Myers Squibb, 311 Pennington-Rocky Hill Road, Pennington, New Jersey 08534

Received April 7, 2008; E-mail: stuart.lindsay@asu.edu

Protein glycosylation comprises a large family of post-translational modifications in eukaryotic and prokaryotic organisms.[1] Oligosaccharides play specific structural roles, maintaining and modulating effector functions that are physiologically relevant, and can be manipulated to optimize the properties of therapeutic antibodies.[2] N-linked glycosylation pathways involve two ancient and highly conserved enzymatic steps that mediate the conversion of oligomannose glycans to hybrid-type and then to complex-type structures. Control and characterization of this process is essential in the production of antibody-based therapeutics, but conventional methods for characterizing glycosylation require significant amounts of material and do not report on the distribution of oligosaccharides on a molecule by molecule basis. Single molecule recognition imaging microscopy[3] is a modification of atomic-force microscopy in which recognition events between a ligand bound to the probe and its target on the surface are mapped simultaneously with sample topography, producing a map of the distribution of target molecules on the surface. We apply it here to visually map the extent of the high-mannose modification on a human IgG_4 monoclonal antibody. In particular, we show that a biologically less effective variant of this antibody has a significant amount of high-mannose species whereas the functional molecule shows limited levels of high-mannose glycoform.

The control IgG molecule used in the study had G0, G1, and G2 structures, as detected using ESI-MS analysis, typical for human IgG molecules. Further, MS analysis also revealed that this control IgG normally contains only a minor amount of mannose 5 (Man5). The trimannose cores of G0 (no terminal galactose), G1 (1 terminal galactose), and G2 (2 terminal galactose) are not accessible to the AFM tip, so normal IgG molecules did not yield a signal. However, MS analysis of the IgG species detected using the MNA-M lectin showed an atypical amount of Man5 variant, >10% Man5, thus rendering it capable of being detected in this study.

Force curves have been recorded using lectins to probe cell surfaces,[4,5] but they have not previously been used in recognition imaging. Successful recognition imaging requires a ligand that has (a) a binding time much less than the time the probe spends scanning over a target on the surface and (b) adequate specificity at the high effective concentration under the scanning probe.[3] We found MNA-M lectin (EY Laboratories, Inc.) to be the most effective of the commercially available lectins for mannose that we tried.

MNA-M lectins were thiolated with *N*-succinimidyl 3-(acetylthio)propionate (SATP, Sigma Inc.) and purified in a PD-10 column (Amersham Pharmacia Biotech). Silicon nitride cantilever tips (Microlever, Veeco, Santa Barbara, CA, coated for MacMode AFM by Agilent Technologies, Chandler, AZ) were aminated as previously described[3] and reacted with a PEG cross-linker of MW = 2700 (from Agilent, Chandler, AZ) using triethylamine and $CHCl_3$. The SATP-labeled lectins were then bound to the PEG cross-linkers with NH_2OH (Sigma) in NaCl/Phosphate buffer. The probes were rinsed in PBS buffer and stored at 4 °C until use.

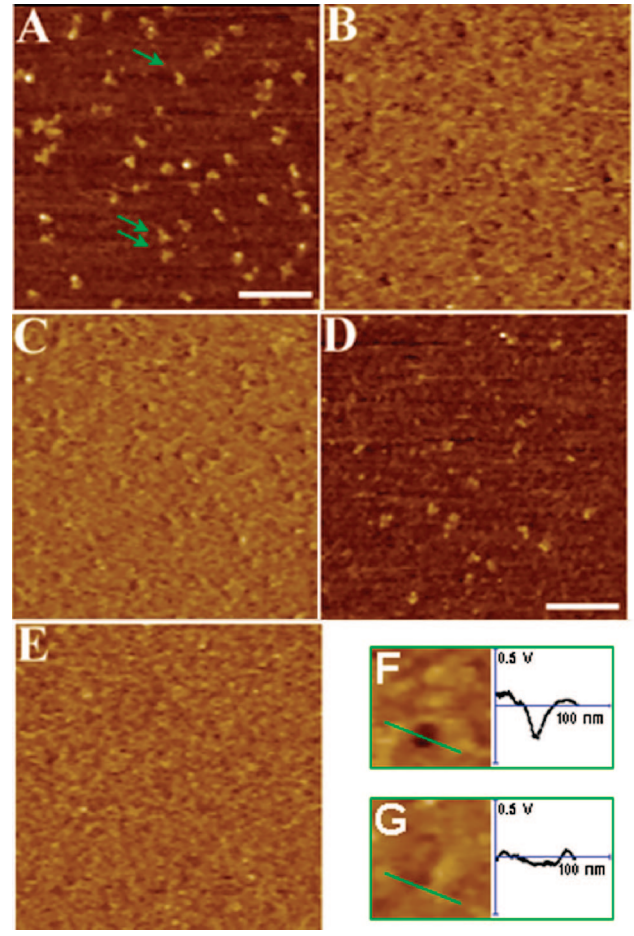

Figure 1. (A) Topographic image of variant IgG_4 molecules (light spots). Scale bar is 150 nm. (B) Corresponding mannose recognition image (dark spots); nearly half the molecules give a positive signal. (C) Repeat scans after blocking with free mannose in solution. The signal is abolished (D) normal IgG_4 molecules (sample E) the corresponding mannose recognition image showing that mannose is not evident on the surface of the normal antibody. Panels (F) and (G) show line scans over a recognition feature before and after blocking. The magnitude of the signal after blocking is comparable to the background noise.

[†] The Biodesign Institute, Arizona State University.
[‡] Department of Chemistry and Biochemistry, Arizona State University.
[§] Department of Physics, Arizona State University.
[||] Bristol-Myers Squibb.

10.1021/ja802535p CCC: $40.75

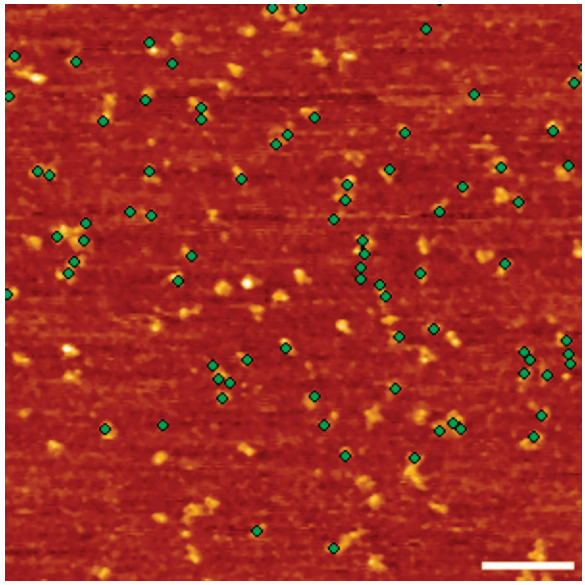

Figure 2. Topographic image of variant IgG_4 molecules with recognition spots superimposed by overlaying them (green dots) on top of the topographic images (light spots). The fraction of the molecules yielding a recognition signals was 47% in a sample of 200 molecules. Scale bar = 150 nm.

The imaging substrate was glutaraldehyde-treated mica prepared as previously described.[6] Immediately after the amino-terminated mica surface was treated with glutaraldehyde, 70 μL of protein solution (0.4 μg/mL) in 10 mM PBS was pipetted onto the treated surface and left for 30 min. The surface was then rinsed again with purified water. The prepared sample was mounted into the SPM liquid flow cell (Agilent, Chandler, AZ) and imaged immediately in 10 mM phosphate buffer (pH 7.5) using a Pico AFM with a PicoTrec recognition imaging attachment (Agilent, Chandler, AZ) with an amplitude between 18 and 20 nm with a set point reduction of 30%. Images of both the variant and the normal IgG_4 molecules are shown in Figure 1, together with the mannose recognition signals (recognition spots appear dark on a light background).

Images of the variant IgG_4 molecules appear normal, many showing the classic "Y" shape expected for an antibody[7] (green arrows on Figure 1A) though the dimensions are somewhat broadened laterally (width = 16 ± 2 nm, length = 26 ± 3 nm) and diminished vertically (height = 1.8 ± 2 nm) compared to the crystal structure owing to tip−sample interactions. The simultaneously acquired mannose recognition image (Figure 1B) shows many recognition features associated with the antibodies (Figure 2), which indicated that high-mannose N-linked oligosaccharides were present on the sample. When free mannose was injected into the flow cell and the same area scanned again, these features were abolished, confirming specificity of the response (Figure 1C). In contrast, scans of the normal IgG_4 molecules (panel D, topography, C recognition, Figure 1) showed no features associated with mannose. Small residual features are thermal noise (cf., Figure 1F,G). These data are typical of what was observed in several repeated runs.

Approximately half of the variant antibodies captured on the substrate surface gave a recognition signal for mannose. It is not clear to what extent this reflects a failure of the recognition process

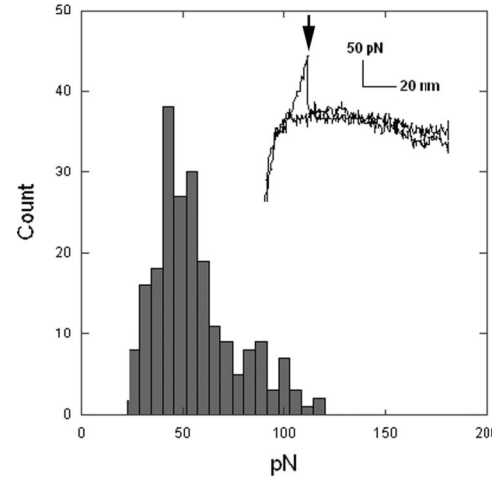

Figure 3. Distribution of peak pull-off forces for MNA-M lectin tethered to an AFM probe with a PEG linker over a dense layer of the variant anti-CD137 molecules. A typical approach and retraction curve is shown in the inset.

(e.g., the target was hidden) versus a heterogeneous mix of antibodies with and without oligomannose species present on the antibody. However, the presence of mannose on the variant IgG_4 was confirmed by intact heavy chain mass analysis, and the population of mannose 5 moiety detected in the variant IgG_4 was about 20%. Since AFM analyzes smaller amounts of material compared with bulky analysis by mass spectrometry, this may explain the difference in the percentage of oligomannose detected.

We confirmed the difference in interaction of the MNA-M-functionalized probe with the two types of antibody by taking force curves over surfaces modified with dense monolayers so that each retraction curve would result from an interaction with a target molecule. A typical approach−retraction curve is shown in the inset of Figure 3, showing a characteristic single-molecule adhesion peak pointed to by the arrow. A histogram of the peak adhesion forces (Figure 3) shows a peak value of about 50 pN, similar in value to the force reported by Lekka et al.[5] for lectin interactions with cell surfaces at a similar loading rate. In contrast, the controls showed only nonspecific adhesion lacking the characteristic feature owing to stretching of the PEG tether.

In summary, we have demonstrated that a lectin may be used to recognize glycosylation on single molecules. Furthermore, we have shown how individual normal and aberrant antibodies can be distinguished on the basis of their glycosylation. This capability further extends the usefulness of the AFM platform in biology.

References

(1) Gabius, H. J.; Andre, S.; Kaltner, H.; Siebert, H. C. *Biochim. Biophys. Acta* **2002**, *1572*, 165–177.
(2) Arnold, J. N.; Wormald, M. R.; Sim, R. B.; Rudd, P. M.; Dwek, R. A. *Annu. Rev. Immunol.* **2007**, *25*, 21–50.
(3) Stroh, C.; Wang, H.; Bash, R.; Ashcroft, B.; Nelson, J.; Gruber, H.; Lohr, D.; Lindsay, S.; Hinterdorfer, P. *Proc. Natl. Acad. Sci. U.S.A.* **2004**, *101*, 12503–12507.
(4) Grandbois, M.; Dettmann, W.; Benoit, M.; Gaub, H. E. *J. Histochem. Cytochem.* **2000**, *48*, 719–724.
(5) Lekka, M.; Laidler, P.; Labedz, M.; Kulik, A. J.; Lekki, J.; Zajac, W.; Styachura, Z. *Chem. Biol.* **2006**, *13*, 505–512.
(6) Wang, H.; Bash, R.; Yodh, J. G.; Hager, G. H.; Lohr, D.; Lindsay, S. M. *Biophys. J.* **2002**, *83*, 3619–3625.
(7) Paulo, A. S.; García, R. *Biophys. J.* **2000**, *78*, 1599–1605.

JA802535P